RSC Advances

ROYAL SOCIETY OF CHEMISTRY

www.rsc.org/advances

Cite this: DOI: 10.1039/c0xx00000x

www.rsc.org/xxxxxx

ARTICLE TYPE

Nanoscale Phase Separation in Bulk Heterojunction Structure of Perylene Bisimide and Porphyrin by Controlling Intermolecular Interactions

Yunan Zhang,[a,b] Wenqiang Zhang,[a] Li Nian,[a] Yuyu Pan,[b] Zengqi Xie,*[a] Linlin Liu,[a] Yuguang Ma*[a,b]

Received (in XXX, XXX) Xth XXXXXXXXX 20XX, Accepted Xth XXXXXXXXX 20XX
DOI: 10.1039/b000000x

We demonstrate the concept of controlling phase separation behavior through designing directional intermolecular interactions. The twisted molecular configuration and intermolecular hydrogen bonds endow **PBI-1** self-assembly into nanofiber aggregates on order of tens of nanometers. In the blend of **Zn-mTNP** and **PBI-1**, the charge transfer interaction was suppressed effectively due to the unfavored π-π stacking for their twisted and planar molecular configurations. The spin-coated films of **Zn-mTNP**, **PBI-1** and their blend have been characterized by UV-vis absorption spectra, and atomic force microscopy, revealing that preferred phase separation structures in nano scale was obtained.

Introduction

Solution-processed small molecules for organic photovoltaics (OPVs) combine the advantages of high purity, defined molecular structure and a more easily reproducible synthesis over conjugated polymer systems.[1, 2] The morphology of bulk heterojunction (BHJ) solution-processed small molecule OPVs is crucial for efficient charge separation and transport.[3, 4] Bicontinuous phases with domain size on order of several nanometers to tens of nanometers, matching the effective exciton diffusion length, could be described as the favorable morphology.[5] The morphology in terms of degree of phase separation and crystallinity (or aggregation) is intrinsically related to the thermodynamic miscibility between donor or acceptor materials, solvent-solute interactions, intrinsic crystallinity (or aggregation) of the active materials.[6, 7] Generally in the polymer/fullerene based BHJ solar cells, the morphology is usually tuned by adjusting the aggregates of donor polymer through comprehensive optimization of regioregularity, molecular weight, donor/acceptor ratio, choice of solvent, annealing conditions and additives, since it is hard for fullerene to form ordered aggregates.[8] However, there are too many uncertainties to design a proper polymer structure easily, considering the high molecular weight distribution and complicated molecular configuration.

Perylene bisimides (PBIs) are promising candidates as non-fullerene acceptor materials[9-13] because, firstly, PBIs are n-type organic semiconductors with high chemical, thermal, and light stabilities;[14, 15] and secondly, PBIs generally show a strong absorption band in the visible region,[16, 17] good electron affinity[13, 14] as well as excellent electron mobility.[18, 19] Furthermore their solubility, optoelectronic and self-assembling properties could be fine-tuned by tailoring the substituted groups.[20, 21] However the traditional unsubstituted PBI derivatives possess a large π planar structure and strong electron affinity, which will lead to either big crystalline aggregates induced by the intermolecular π-stacking interactions,[22, 23] or uniformly dispersed sandwich structures at the molecular level induced by the charge transfer (CT) interactions[24] of donors and acceptors. Recently Zhan et. al.[25] successfully tuned the aggregates of PBI in the polymer/PBI system by introducing a dimer of PBIs linked by the bridge thienyl, giving a promising power conversion efficiency (PCE) of 4.03% under illumination with AM 1.5G simulated solar light at 100 mW cm^{-2}.

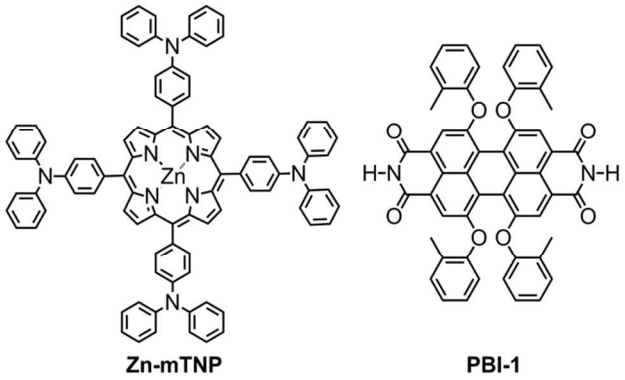

Scheme 1. Structure of porphyrin and perylene bisimide.

Herein we demonstrate the concept of controlling phase separation behavior through designing directional intermolecular interactions. The chosen acceptor material **PBI-1** (Scheme 1) possesses a twist molecular configuration bearing two N-H groups at the tip of the molecular structure, which induces the formation of J-aggregate stacking arrangement into one-dimensional nanofiber as reported previously.[26] The donor material **Zn-mTNP** (Scheme 1) shows a planar core structure

incorporated four flexible triphenylamine peripheral substituents and Zn (II) ion in the centre. We observed that the blend of **PBI-1** and **Zn-mTNP** tend to form nano-structured phase separation, which is attributed to the proper design of the intermolecular interactions, i.e. preferred PBI-PBI H-bonding interactions and porphyrin-porphyrin π-π interactions, but prohibited PBI-porphyrin CT interaction for the unfavored π-stacking due to twisted and planar molecular structures of them.

Experimental Section

Characterization and Measurements.

UV-vis was recorded on a Shimadzu UV-3100 spectrophotometer using 1 cm path length quartz cells. Electrochemical measurements were performed with a BAS 100W Bioanalytical System: a glass-carbon disk electrode was used as the working electrode, a Pt wire as the counter electrode, Ag/Ag^+ as the reference electrode with ferrocene as the internal standard and Bu_4NPF_6 (0.1 M) as the electrolyte in acetonitrile. The reductive and oxidative onset potentials were used to estimate the orbital energies and band gaps.[27] The HR-TEM experiment was performed by using a JEOL model JEM-3010 with an acceleration voltage of 300 kV. The atomic force microscopy (AFM) images are recorded on a Seiko SPA 400 with an SPI 3800 probe station for tapping mode and on NanoScope NS3A system (Digital Instrument) for contact mode.

Materials.

The synthesis of **PBI-1** and **Zn-mTNP** were synthesized according to the literatures.[26, 28] Solvents and reagents were purchased from commercial sources, unless otherwise stated, and purified and dried according to standard procedures. ITO substrates with a sheet resistance of 15 Ω sq^{-1} were purchased from CSG HOLDING Co., LTD (Shenzhen, P. R. China), while PEDOT: PSS (Clevios P AI4083) was purchased from H.C. Starck Clevios.

Device Fabrication.

The OPV device structure was ITO/poly(3,4-ethylenedioxy-thiophene):poly(styrene sulfonate) (PEDOT:PSS)/porphyrin: perylene bisimide (by weight)/poly[(9,9-bis(3-(N,N-dimethyl-amino)propyl)-2,7-fluorene)-alt-2,7-(9,9–dioctylfluorene)] (PFN) /Al. ITO-coated glass substrates were pre-cleaned by sonication in acetone, detergent, distilled water, and isopropyl alcohol. After oxygen plasma cleaning for 4 min, a 40-nm-thick PEDOT:PSS (Bayer Baytron 4083) anode buffer layer was spin-coated onto the ITO substrate, and then dried by baking in a vacuum oven at 120 °C for 20 min. The porphyrin: perylene bisimide active blend layer, with thickness of ~ 80 nm, was prepared by spin-coating the tetrahydrofuran solutions. Subsequently, an ultra-thin PFN layer was deposited by spin-coating (2000 rpm for 30 s) from 0.02% (w/v) solution in methanol. The thicknesses of these organic films were determined by the surface profiler (Tencor Alfa-Step 500). A 90 nm aluminum (Al) layer was evaporated through a shadow mask to define the active area of the devices (~2×8 mm^2) and form a top anode, at a base pressure of 1×10^{-4} Pa. The PCE was determined from J– V curve measurements (using a Keithley 2400 sourcemeter) under 1 sun, AM 1.5G (air mass 1.5 global) spectrum from a solar simulator (Oriel model 91192) (100 mW cm^{-2}).

Results and Discussion

Theoretical Calculation.

PBI-1 bears two N-H groups at the imide positions and four bay-area phenoxy substituents. The molecule possess a twisted structure with perylene core twisting angle of ~30° as optimized by density functional theory (DFT) at the B3LYP/6-31G level by using the Gaussian 09 Package,[29] which is due to the four bulky bay-area substituents. The twisted molecular structure prohibits the sandwich-type face-to-face π-stacking, but the intermolecular hydrogen bonds drive self-assembly into slipped J-aggregate stacking arrangement (Scheme 2a). The molecular configuration of **Zn-mTNP** was also calculated that shows a planar porphyrin core structure, which will allow formation of sandwich-type molecular stacking through the intermolecular π-π interactions (Scheme 2b).

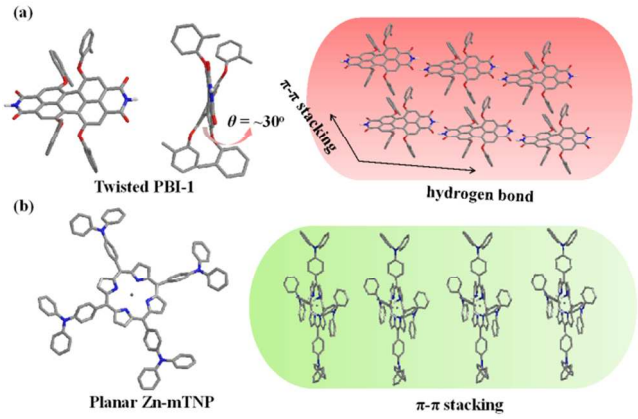

Scheme 2 Optimized geometries and schematic formation of aggregates of (a) **PBI-1** and (b) **Zn-mTNP**.

To further understand the electronic properties, the three-dimensional geometries and the frontier molecular orbital energy levels was also calculated at the B3LYP/6-31G level by using the Gaussian 09 Package (Figure 1). In case of **PBI-1**, both highest occupied molecular orbital (HOMO) and lowest unoccupied molecular orbital (LUMO) were mainly localized on the perylene bisimide moieties. In the self-assembled nanofiber aggregates, the exciton/electron transfer along the slipped J-aggregate (long axis of the fiber) would be totally allowed. As for **Zn-mTNP**, the HOMO localize on the whole molecule, while the LUMO mainly localize on the porphyrin core structure. In the sandwich-type molecular stacking, the exciton and charge transfer along the π-π stacking direction could be facilitated.

Photophysical Properties

In the UV/Vis absorption spectra of films measured on quartz substrates (Figure 2), **Zn-mTNP** showed a strong absorption at around 450 nm and two weak ones at 583 and 635 nm, which were the typical Soret and Q bands absorption of porphyrin core, respectively.[30, 31] The absorption at 350 nm was attributed to the typical absorption of triphenylamine.[28, 32, 33] **PBI-1** exhibited a sharp absorption band at 650 nm that was ascribed to the formation of J-aggregate.[26] The strong absorption in red-light

region made **PBI-1** a promising light absorber for OPVs.

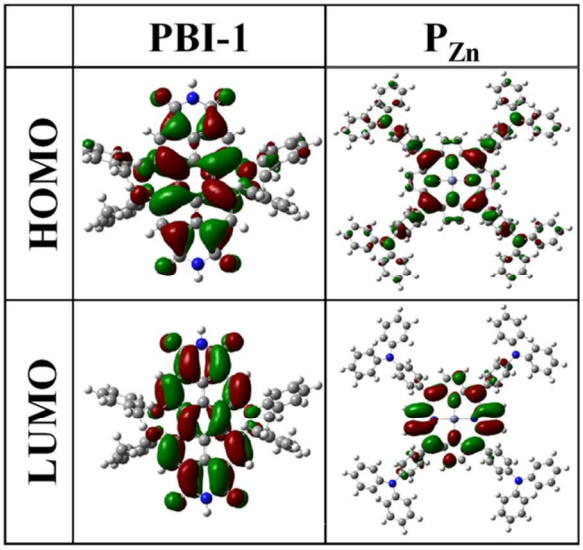

Fig.1 Calculated HOMO and LUMO density maps of **PBI-1** and **Zn-mTNP.**

For the blended film of **PBI-1** and **Zn-mTNP**, there were typical absorption bands of **PBI-1** J-aggregates and **Zn-mTNP** film in the absorption spectra. Note that the typical absorption of J-aggregate of PBI-1 lying at 650 nm appeared in the absorption spectra of blended films, suggesting that **Zn-mTNP** molecule would not impair the J-aggregate of **PBI-1** by imbedding into between PBI-1 molecules. Meanwhile the long-range absorbance from 350 to 700 nm, covering the whole range of visible light, ensured the further applications of **PBI-1** and **Zn-mTNP** in OPVs.

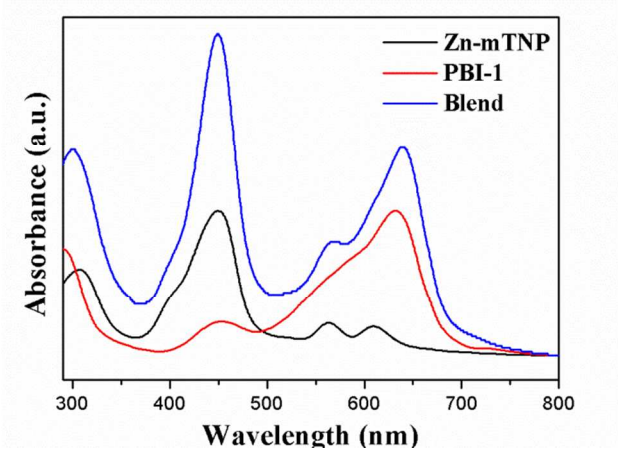

Fig.2 UV/Vis absorption spectra of the thin films of **PBI-1**, **Zn-mTNP** and their blend (w/w 1:1).

Morphology Investigation

Atomic force microscopy (AFM) measurements were carried out to investigate the surface morphology of **PBI-1**, **Zn-mTNP** and their blend films. As shown in Figure 3a-b, there were typical nanofiber aggregates with domain size of around 20-40 nm in **PBI-1** film from 2 mg mL^{-1} THF solutions, while the film of **Zn-mTNP** from 8 mg mL^{-1} THF solution showed very smooth surface (RMS < 1 nm). In blended film (Figure 3c-d), typical nanofiber aggregates remained almost the same with that in **PBI-1** film, indicating that addition of **Zn-mTNP** would not impair aggregates of **PBI-1**. Moreover nanofibers of **PBI-1** overlapped each other to form the continuous interpenetrating networks filled with porphyrins, beneficial for achieving preferable bicontinuous phase separation structure in OPVs.

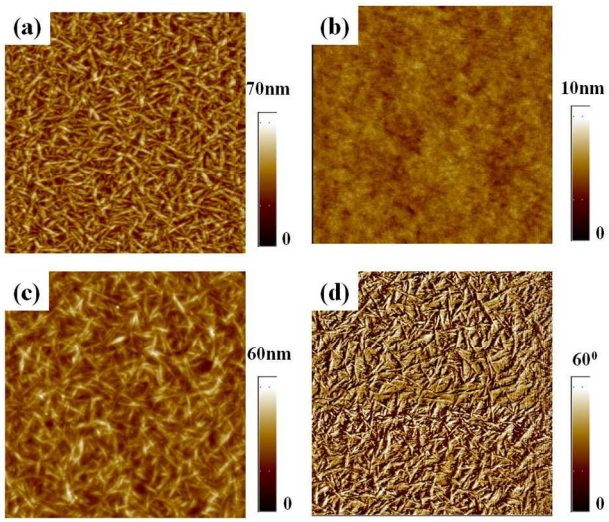

Fig.3 AFM height images of **PBI-1** (a), **Zn-mTNP** (b), and **PBI-1/Zn-mTNP** blends (c), and AFM phase image of **PBI-1/Zn-mTNP** blends (d). All the samples were spin-coated from THF solution onto ITO substrates.

To further confirm aggregates of **PBI-1** after blended with **Zn-mTNP**, more blended films with different ratio (**PBI-1**: **Zn-mTNP** = 1:9 and 3:7) were fabricated and characterized (Figure S2). As the content of **PBI-1** was increased, the typical nanofiber aggregates of **PBI-1** enlarged both in width and length, which clearly indicated that nanofiber-like aggregates in blended films could be attributed to **PBI-1**.

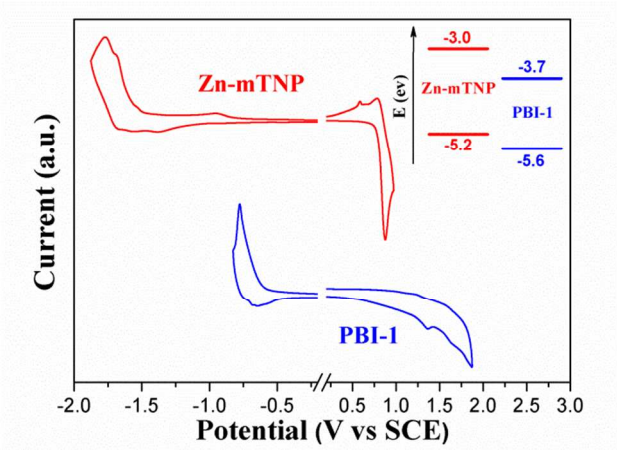

Fig.4 Caption Cyclic voltammograms of **PBI-1** and **Zn-mTNP**. Inset: Energy level diagrams for **PBI-1** and **Zn-mTNP**.

Organic Photovoltaic Devices

Electrochemical properties of **Zn-mTNP** and **PBI-1** were investigated by cyclic voltammetry (CV) as shown in Figure 4. The HOMO and LUMO of **Zn-mTNP** were calculated to be -5.2 eV and -3.0 eV, and that of **PBI-1** were -5.6 eV and -3.7 eV.[27]

From the energy level diagram, it is clear that the difference between HOMO of Zn-mTNP and LUMO of PBI-1 (1.5 eV) is smaller than the excitation energies of Zn-mTNP (1.83 eV) and PBI-1 (1.80 eV), which indicates the highly favoured intermolecular charge-transfer process. [34]

BHJ OPVs were fabricated with a general device structure of ITO/PEDOT:PSS/**Zn-mTNP**:**PBI-1**/PFN/Al and were measured under AM 1.5 illumination, 100 mW cm^{-2} (Figure S4). The incorporation of an ultrathin polymeric PFN layer as a cathode interlayer in bulk heterojunction solar cells has been reported to improve the electron injection/extraction contact.[35, 36] The device performance was firstly explored by blending **Zn-mTNP** with **PBI-1** at different ratios ranging from 5:5 to 9:1 in THF (Table S1). The optimized weight ratio of **Zn-mTNP** with **PBI-1** is found to be 4:1, yielding a PCE of 0.22% with an open-circuit voltage (Voc) of 1.03 V, a short-circuit current (Jsc) of 0.93 mA cm^{-2} and a fill factor (FF) of 23%, and the typical current density–voltage (J–V) characteristics are shown in Figure S5.

Conclusions

In conclusion, we have demonstrated that the morphology of the BHJ layer can be effectives controlled by the rational molecular design for donor and acceptor materials. By adjusting the supramolecular interactions including hydrogen bond and π-stacking of **PBI-1**, nanoscale fiber-like J-aggregates had been fabricated. When blended with **Zn-mTNP** in the as-prepared BHJ OPVs, ordered nanoscale phase separation had been obtained by the self-assembly of **PBI-1**. Though the OPV performance is still not satisfying, the result reported here clearly provide new perspectives to achieve preferred phase separation in BHJ OPVs.

Acknowledgements

We thank the supports from the Natural Science Foundation of China (51373054), National Basic Research Program of China (973 Program) (2014CB643504), Fundamental Research Funds for the Central Universities (2013ZZ0001), Guangdong Natural Science Foundation (S2012030006232), and Introduced Innovative R&D Team of Guangdong (201101C0105067115).

Notes and references

[a] *Institute of Polymer Optoelectronic Materials and Devices, State Key Laboratory of Luminescent Materials and Devices, South China University of Technology, Guangzhou 510640, P. R. China. E-mail: ygma@scut.edu.cn, msxiez@scut.edu.cn*

[b] *State Key Laboratory of Supramolecular Structure and Materials, Jilin University, Changchun 130012, P. R. China.*

† Electronic Supplementary Information (ESI) available: [TEM and AFM image of PBI-1 aggregates, AFM height images of blend films, Cyclic voltammograms of PBI-1 and Zn-mTNP, Schematic illustration of the device structure, J-V curves of OPVs, Photovoltaic properties of OPVs]. See DOI:10.1039/b000000x/

1. O. P. Lee, A. T. Yiu, P. M. Beaujuge, C. H. Woo, T. W. Holcombe, J. E. Millstone, J. D. Douglas, M. S. Chen and J. M. J. Fréchet, *Adv. Mater.*, 2011, **23**, 5359-5363.
2. J. Zhou, X. Wan, Y. Liu, G. Long, F. Wang, Z. Li, Y. Zuo, C. Li and Y. Chen, *Chem. Mater.*, 2011, **23**, 4666-4668.
3. C. J. Brabec, M. Heeney, I. McCulloch and J. Nelson, *Chem. Soc. Rev.*, 2011, **40**, 1185-1199.
4. H. Hoppe and N. S. Sariciftci, *J. Mater. Chem.*, 2006, **16**, 45-61.
5. N. Cho, H.-L. Yip and A. K. Y. Jen, *Appl. Phys. Lett.*, 2013, **102**, 233903-233904.
6. M. He, W. Han, J. Ge, Y. Yang, F. Qiu and Z. Lin, *Energ. Environ. Sci*, 2011, **4**, 2894-2902.
7. M. He, F. Qiu and Z. Lin, *J. Mater. Chem.*, 2011, **21**, 17039-17048.
8. M. T. Dang, L. Hirsch, G. Wantz and J. D. Wuest, *Chem. Rev.*, 2013, **113**, 3734-3765.
9. I. A. Howard, F. Laquai, P. E. Keivanidis, R. H. Friend and N. C. Greenham, *J. Phys. Chem. C*, 2009, **113**, 21225-21232.
10. L. Schmidt-Mende, A. Fechtenkötter, K. Müllen, E. Moons, R. H. Friend and J. D. MacKenzie, *Science*, 2001, **293**, 1119-1122.
11. C. W. Tang, *Appl. Phys. Lett.*, 1986, **48**, 183-185.
12. X. Zhan, Z. a. Tan, B. Domercq, Z. An, X. Zhang, S. Barlow, Y. Li, D. Zhu, B. Kippelen and S. R. Marder, *J. Am. Chem. Soc.*, 2007, **129**, 7246-7247.
13. Y. Zhou, Q. Yan, Y.-Q. Zheng, J.-Y. Wang, D. Zhao and J. Pei, *J. Mater. Chem. A*, 2013, **1**, 6609-6613.
14. M. R. Wasielewski, *J. Org. Chem.*, 2006, **71**, 5051-5066.
15. F. Wurthner, *Chem. Commun.*, 2004, 1564-1579.
16. D. Ke, C. Zhan, S. Xu, X. Ding, A. Peng, J. Sun, S. He, A. D. Q. Li and J. Yao, *J. Am. Chem. Soc.*, 2011, **133**, 11022-11025.
17. E. Krieg, H. Weissman, E. Shirman, E. Shimoni and B. Rybtchinski, *Nat Nano*, 2011, **6**, 141-146.
18. Y. Che, A. Datar, X. Yang, T. Naddo, J. Zhao and L. Zang, *J. Am. Chem. Soc.*, 2007, **129**, 6354-6355.
19. A. Lv, S. R. Puniredd, J. Zhang, Z. Li, H. Zhu, W. Jiang, H. Dong, Y. He, L. Jiang, Y. Li, W. Pisula, Q. Meng, W. Hu and Z. Wang, *Adv. Mater.*, 2012, **24**, 2626-2630.
20. B. A. Jones, A. Facchetti, M. R. Wasielewski and T. J. Marks, *J. Am. Chem. Soc.*, 2007, **129**, 15259-15278.
21. M. C. R. Delgado, E.-G. Kim, D. A. d. S. Filho and J.-L. Bredas, *J. Am. Chem. Soc.*, 2010, **132**, 3375-3387.
22. V. Kamm, G. Battagliarin, I. A. Howard, W. Pisula, A. Mavrinskiy, C. Li, K. Müllen and F. Laquai, *Adv. Energy. Mater.*, 2011, **1**, 297-302.
23. E. Zhou, J. Cong, Q. Wei, K. Tajima, C. Yang and K. Hashimoto, *Angew. Chem.*, 2011, **123**, 2851-2855.
24. H.-C. Lin and B.-Y. Jin, *Materials*, 2010, **3**, 4214-4251.
25. X. Zhang, Z. Lu, L. Ye, C. Zhan, J. Hou, S. Zhang, B. Jiang, Y. Zhao, J. Huang, S. Zhang, Y. Liu, Q. Shi, Y. Liu and J. Yao, *Adv. Mater.*, 2013, **25**, 5791-5797.
26. Z. Xie, V. Stepanenko, B. Fimmel and F. Wurthner, *Mater. Horiz.*, 2014, **1**, 355-359.
27. A. P. Kulkarni, C. J. Tonzola, A. Babel and S. A. Jenekhe, *Chem. Mater.*, 2004, **16**, 4556-4573.
28. S. Fu, X. Zhu, G. Zhou, W. Y. Wong, C. Ye, W. K. Wong and Z. Li, *Eur. J. Inorg. Chem.*, 2007, **2007**, 2004-2013.
29. M. Frisch, G. Trucks, H. Schlegel, G. Scuseria, M. Robb, J. Cheeseman, G. Scalmani, V. Barone, B. Mennucci and G. Petersson, *Inc., Wallingford CT*, 2009.
30. M. Gouterman, *J. Mol. Spectrosc.*, 1961, **6**, 138-163.
31. M. Gouterman, G. H. Wagnière and L. C. Snyder, *J. Mol. Spectrosc.*, 1963, **11**, 108-127.
32. C. W. Huang, K. Y. Chiu and S. H. Cheng, *Dalton Trans.*, 2005, 2417-2422.
33. C. Y. Huang, C. Y. Hsu, L. Y. Yang, C. J. Lee, T. F. Yang, C. C. Hsu, C. H. Ke and Y. O. Su, *Eur. J. Inorg. Chem.*, 2012, **2012**, 1038-1047.
34. P. Peumans, A. Yakimov and S. R. Forrest, *J. Appl. Phys.*, 2003, **93**, 3693-3723.
35. Z. He, C. Zhong, X. Huang, W. Y. Wong, H. Wu, L. Chen, S. Su and Y. Cao, *Adv. Mater.*, 2011, **23**, 4636-4643.
36. Z. He, C. Zhong, S. Su, M. Xu, H. Wu and Y. Cao, *Nat. Photonics*, 2012, **6**, 593-597.